Transport Phenomena in Electric Smelting of Nickel Matte: Part I. Electric Potential Distribution

Y.Y. SHENG, G.A. IRONS, and D.G. TISDALE

An electric potential probe was constructed so that simultaneous, multiple measurements of electric potential could be made in a six-in-line electric furnace for smelting nickel calcine having a maximum transformer capacity of 36 MVA. When the electric potential distributions were compared with those calculated from the solution of the Laplace equation, it was evident that there was significant electric potential drop at the electrode surface, 100 to 120 V for an applied potential of 180 to 230 V and currents of 20 to 30 kA. The Soderberg electrodes were continuously oxidized in the slag, likely creating carbon monoxide. The electric potential drop at the surface was attributed to arcing through the carbon monoxide. Thus, heat was released in the immediate vicinity of the electrode due to arcing, as well as in the bulk of the slag by Joule heating. The proper distribution of heat dissipation is required for the transport model, developed in Part II of this series.

I. INTRODUCTION

ELECTRIC smelting is used for a wide variety of materials such as copper, nickel calcine, nickel laterites, steel, prereduced iron ore, and electric arc furnace dust. There are at least four distinct smelting techniques.[1]

(1) In immersed-electrode smelting, the electrode tips are dipped into molten slag, where electrical energy is generated by Joule heating. This practice is employed mainly for copper-nickel calcines and nickel laterites. The present study focuses on this practice.
(2) Open-arc smelting uses an arc between the electrode and the bath to generate heat. This technique is most commonly used for melting metals such as steel. It is important that the heat radiated by the arc be captured by the melt; the development of foaming slag practices has improved the energy recovery in modern ultra-high-power furnaces.
(3) Submerged-arc smelting is the traditional method for reduction smelting with coke in furnaces producing ferroalloys, silicon, and phosphorus. Electric energy is liberated by arcing between coke particles floating on the bath.
(4) Shielded-arc smelting was developed in Falconbridge's Dominican Republic operations for laterite smelting. Long arcs are covered with charge to ensure efficient use of electrical energy for smelting.[1]

Most of the world's nickel is produced either by flash smelting or by electric smelting.[2] The major advantages of the electric smelting processes are the high sulfur capture and high metal recoveries.[3] This process requires large amounts of electric energy, which is often the most costly purchased consumable. For example, the Falconbridge furnace modeled in the present study is the single largest load on the public utility grid in Ontario, Canada. Consequently, even small improvements in electrical use can have enormous environmental and financial benefits. Surprisingly, there have been few published studies of electrical power use in electric furnaces, as will be reviewed in Section II. This lack of understanding has prompted the present study.

In Part I of this two-part article, the electric potential distribution inside a full-scale operating furnace was measured. The measurements revealed a substantial electric potential drop in the immediate vicinity of the electrodes, which had not been previously reported. The electric potential distribution is one of the most important factors in determining the heat use distribution. In Part II, this information is used to develop a comprehensive model for fluid flow, heat transfer, and electric current distribution in Falconbridge's electric furnace.[4]

II. LITERATURE REVIEW

In immersed-electrode smelting furnaces, heat is supplied to the bath by an alternating current flowing between electrodes immersed in the molten slag. The heat generation and transfer process is determined by the electrical conductivity of the molten slag and the electric potential applied to electrodes, as well as the specific geometry of the furnace, which is represented by a geometric factor defined by the following equation:[5,6]

$$R_s = \frac{f_g}{\sigma_s} \qquad [1]$$

where R_s is the total resistance between two electrodes, σ_s is the electrical conductivity of slag, and f_g is the geometric factor. To date, most efforts have concentrated on the determination of appropriate algebraic expressions for the geometric factor in various furnace configurations. Urquhart *et al.*[7] investigated the electrical characteristics of the Cu-Ni electric smelting process by measuring slag temperature, slag composition, and the electrical parameters. They also conducted experiments with small-scale analog models

Y.Y. SHENG, formerly Post Doctoral Fellow with the Department of Materials Science and Engineering, McMaster University, is Research Scientist, Noranda Technology Centre, Pointe Clairs, PQ, Canada H9R 1G5. G.A. IRONS, DOFASCO/NSERC Professor of Process Metallurgy, is with the Department of Materials Science and Engineering, McMaster University, Hamilton, ON, Canada L8S 4L7. D.G. TISDALE, Process Engineer, is with the Smelter Complex, Falconbridge Limited, Falconbridge, ON, Canada P0M 1S0.

Manuscript submitted April 12, 1996.

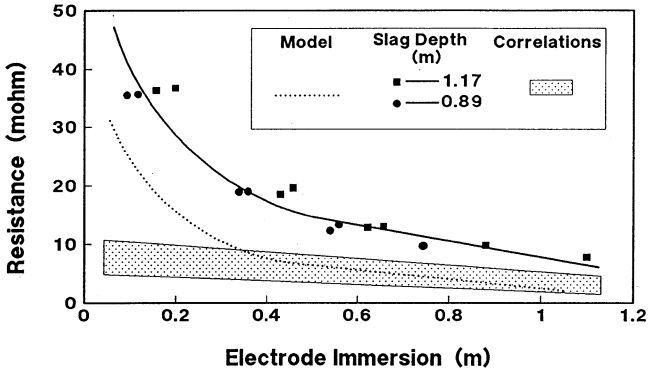

Fig. 1—Measured resistance between electrodes in the Falconbridge electric furnace as a function of electrode immersion for two different slag depths.[9] The hatched region shows that the previous correlations[6,7,8] underestimate the resistance. The dotted line is the ohmic resistance of the slag calculated in the present work.

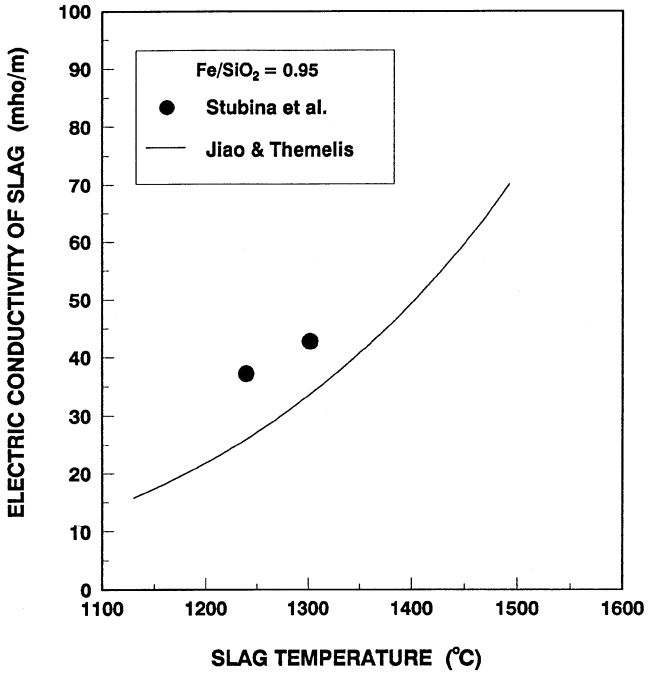

Fig. 2—The electrical conductivity of the slag in the present study with an iron-to-silica ratio of 0.95. Stubina *et al.*[11] measured the conductivity, whereas Jiao and Themelis[10] developed correlations based on measurements.

to study the effect of the electrode geometry on current partition in the slag, and they computed the power generation distribution in the bath with mathematical models based on measured voltage and current data. Again, using analog models, Jiao and Themelis[8] developed their own correlations, which they claimed to cover more electrical current paths and therefore to be more accurate than previous correlations.

These studies have contributed greatly to our understanding of the heat generation and transfer process in an electric furnace. However, in the Falconbridge furnace, it was found that there was a large difference between the measured slag resistance and these correlations,[9] as shown in Figure 1. (Calculations from the present model are also shown for later discussion.) The discrepancy is particularly severe at shallow electrode immersions. Since heat release

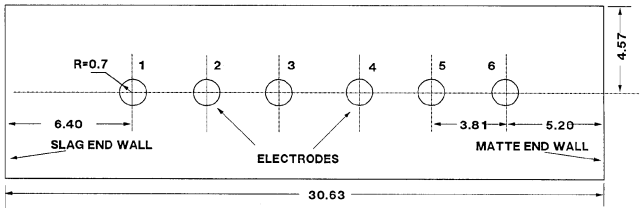

Fig. 3—Plan view of the Falconbridge electric furnace for nickel smelting, showing the internal dimensions in meters.

in the slag follows Ohm's law, misrepresentation of the slag resistance results in an error in the calculated power generation rate in the furnace.

The electrical power release rate is also dependent on the electrical conductivity of slag, which is a strong function of both slag temperature and composition. Recently, Jiao and Themelis[10] proposed some useful correlations for slag conductivity. They carefully analyzed existing data from both laboratory and plant measurements and performed multiple linear regression analyses to relate the slag conductivity to the molar concentrations of Ca^{+2}, Mg^{+2}, and other cations. The electrical conductivity of Falconbridge's electric furnace slag was measured by Stubina *et al.*[11] As Figure 2 shows, the measured conductivities were slightly higher than those from the correlations proposed by Jiao and Themelis. The data and the correlations show a strong dependency of slag conductivity on temperature and on the Fe/SiO_2 ratio of the slag. However, variations in the slag conductivity due to fluctuations in slag composition or temperature cannot account for the large discrepancy in Figure 1 between the measured slag resistance and that calculated using the correlations. Therefore, there are some additional factors that influence the resistance in the furnace. The present experiments were undertaken to comprehend them.

III. PROCESS DESCRIPTION

In 1978, Falconbridge Limited commissioned a new process in Falconbridge, Ontario, which consists of two slurry-fed fluidized-bed roasters for partial sulfur elimination and two electric furnaces for smelting the hot calcine. Cleaned roaster gases are treated in a single-contact acid plant. Matte from the electric furnaces is processed in Peirce–Smith converters. A semifinished matte is shipped to Falconbridge's Norwegian refinery for further treatment.[12] Top and side views of the electric furnace are shown in Figures 3 and 4, respectively. The incoming electric power at 115 kV is stepped down to 13.8 kV in the primary transformer. The electric furnace has three secondary 12 MVA transformers, which are located in vaults adjacent to the furnace and have on-load tap changers to produce voltages between 137 and 254 V in the star connection and between 238 and 440 V in the delta connection. The electrical configuration of the furnace is shown in Figure 5 and other operational parameters are listed in Table I.

IV. MEASUREMENT OF ELECTRIC POTENTIAL DISTRIBUTION IN SLAG

A. *The Electric Potential Probe*

The electric potential distribution in the slag was measured with a newly designed electric potential probe. A sec-

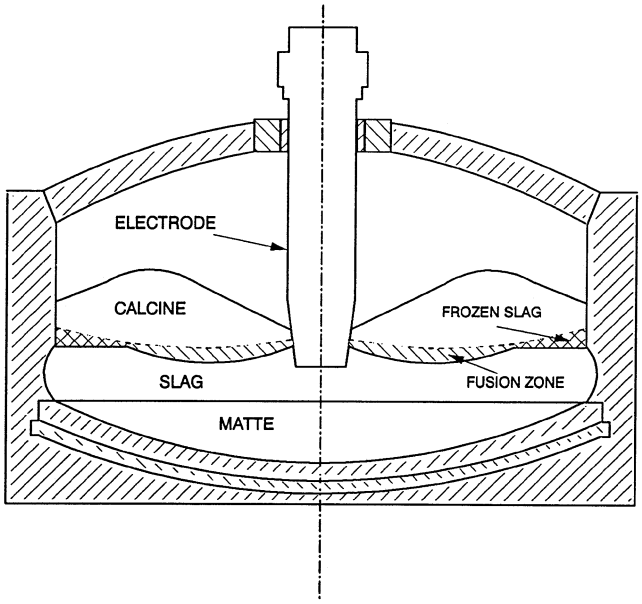

Fig. 4—Schematic end view of the Falconbridge electric furnace for nickel smelting.

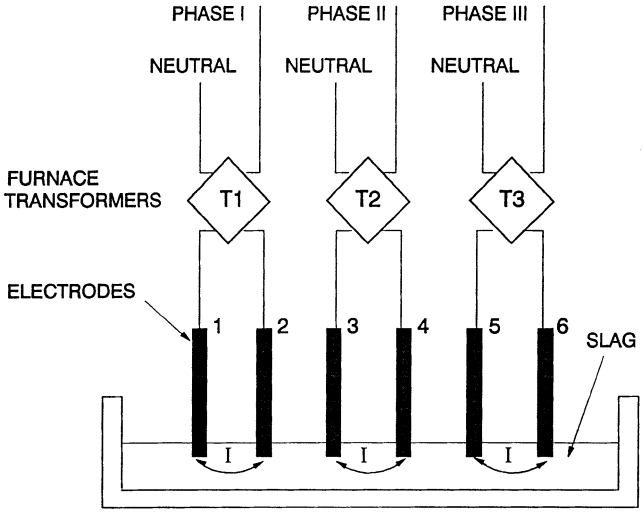

Fig. 5—Electrical circuit of the Falconbridge electric furnace for nickel smelting.

Table I. Electric Furnace Test Conditions

Power (MW)	25 to 40
Electric potential (V)	180 to 230
Current (kA)	20 to 28
Electrode diameter (mm)	1400
Electrode immersion (mm)	200 to 600
Electrode consumption (kg C/tonne calcine)	1 to 1.8 (all six electrodes)
Slag depth (mm)	1200
Matte depth (mm)	900
Slag temperature (°C)	1220 to 1300
Matte temperature (°C)	1150 to 1200

tion of the probe is shown in Figure 6. The probe was made of a steel pipe with an outer diameter of 25.4 mm and a length of 3.0 m. The bottom half of the pipe was covered with a 25.0-mm-thick layer of alumina-rich refractory. Five

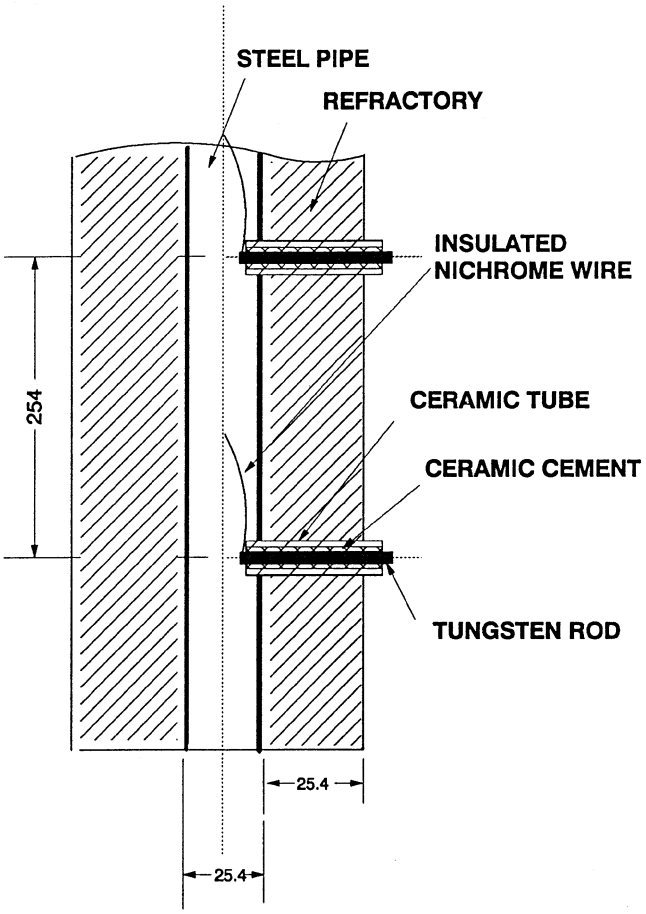

Fig. 6—Cross section of a section of the probe used for the electric potential measurement, showing the details of construction of two of the five tungsten electrodes, not to scale.

electrodes made of tungsten rod with a diameter of 3.18 mm and a length of 44.5 mm were positioned in the refractory and the pipe. The distance between the electrodes was 254 mm. Nichrome alloy wire, protected by a high-temperature ceramic sleeve, was used to connect each electrode to a digital voltmeter. The lowest electrode was immersed just below the matte/slag interface to act as the ground for the electric potential measurement; all measurements are reported with respect to the matte potential.

The temperature distribution in the bath was measured with a separate holding rod containing a K-type thermocouple. The thermocouple had a stainless steel sheath with an outer diameter of 6.35 mm and a length of about 7 m.

B. *The Location of Measurement*

The locations for the electric potential measurement in slag were quite restricted since the furnace was enclosed, except for several ports in the roof for temperature measurement. Two such ports on either side of an electrode were chosen for the electric potential measurement, and their locations relative to the electrode are shown in Figure 7 as locations A and B. Because the probes were inserted at an angle, they sagged if they were inside the furnace for an extended time. To overcome this problem, some measurements were taken vertically downward at location C. The probe assembly was lowered on a carriage to multiple

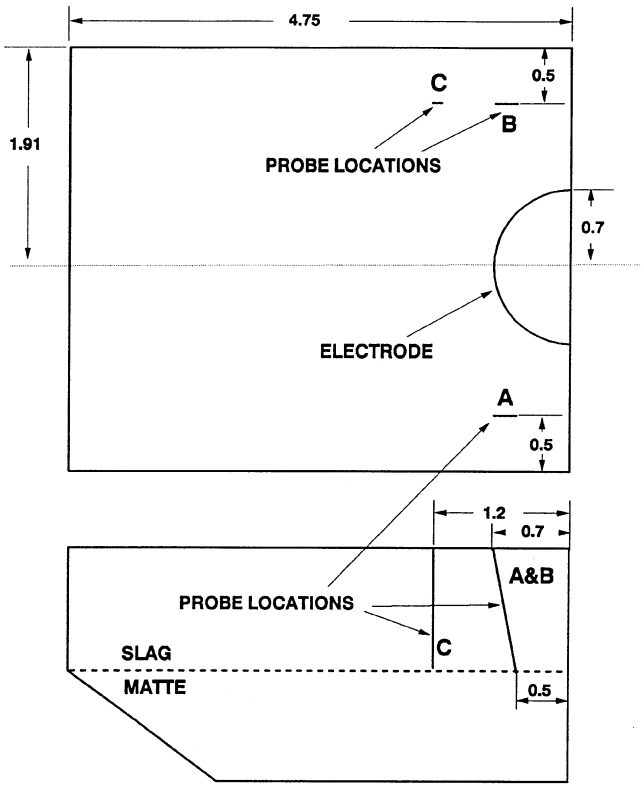

Fig. 7—Plan and end views of the locations for electrical potential measurements. Dimensions are in meters.

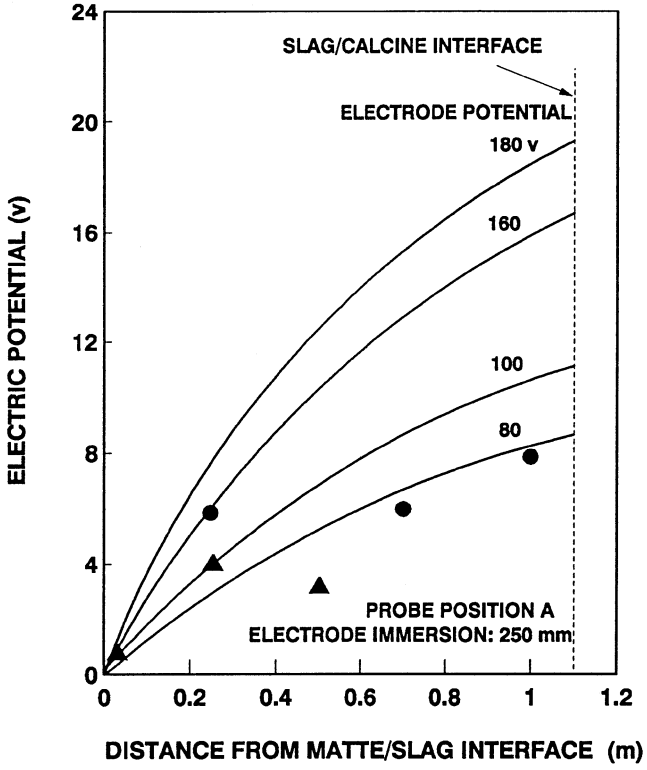

Fig. 8—Electric potential in the slag with respect to the matte as a function of distance from the matte at location A in furnace 1. ● Data correspond to 180 and 130 V applied to electrodes 1 and 2, respectively, 28 kA, and 8.7 MW between electrodes 1 and 2 with a slag depth of 250 mm. ▲ Data correspond to 230 and 180 V applied to electrodes 1 and 2, respectively, 32 kA, and 13 MW between electrodes 1 and 2 with a slag depth of 300 mm. The lines were computed from the model for a slag depth of 250 mm, and the various potentials applied to the slag, V_s, indicated.

positions, so that more than five measurements could be made at each location. The measurements were carried out in furnaces 1 and 2; however, the locations in each furnace were different. In furnace 1, location A (Figure 7) was between electrodes 1 and 2 (phase I, Figure 5). In furnace 2, locations B and C were between electrodes 2 (phase I) and 3 (phase II).

C. *Experimental Procedure*

Preceding the measurements, the furnace was maintained in as steady an operation as possible. The procedure was as follows:

(1) measurement of the immersion of the furnace electrodes by first raising them to the slag-calcine interface (indicated by a zero current reading) and then returning them to the designated positions;
(2) measurement of the vertical temperature profile in slag and matte with the furnace power off at the same locations as the electric potential measurement;
(3) measurement of the depths of furnace bottom buildup, matte, and slag, respectively, at the same locations as the electric potential measurement with a sounding bar; and
(4) electric potential measurement with the electric potential probe.

D. *Experimental Results*

The measured electric potential distributions for three different locations are shown in Figures 8 through 10. The curves superimposed on the diagram are the mathematical model results, which will be discussed in Section V. In each figure, the uppermost curve represents the electric potential profile that would be observed if the electric potential that the slag experiences, V_s, were the electric potential applied to the electrode. Clearly, the measured electric potentials are substantially lower. The other curves represent lower electric potentials for the slag. Note that the electric potentials that the slag experiences are some 100 to 120 V lower than those applied to the electrode.

A temperature profile for location A is shown in Figure 11. The temperature was reasonably uniform, except near the matte interface. The average slag tapping temperature only varied from 1230 °C to 1280 °C in the present experiments. If the power were off for more than 30 minutes for a temperature measurement, then the slag became thermally stratified. The data in Figure 11 were gathered over a period of less than 30 minutes.

V. DISCUSSION

A. *Calculation of Electric Potential Distribution in Slag*

The details of the mathematical model used for the calculation of the electric potential distribution are presented in Part II of this article, where a simplified Maxwell's equation[13,14] is solved together with the flow and temperature fields. As will be shown, the electromagnetic force field is

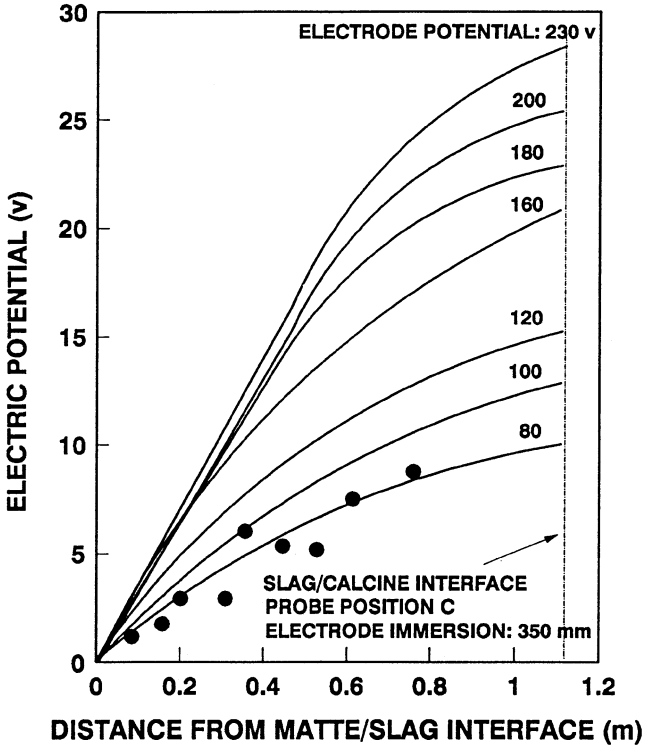

Fig. 9—Electric potential in the slag with respect to the matte as a function of distance from the matte at location C in furnace 2. The data correspond to 230 and 210 V applied to electrodes 2 and 3, respectively, 23 kA, and 12 MW between electrodes 2 and 3 with a slag depth of 300 mm. The lines were computed from the model for a slag depth of 350 mm, and the various potentials applied to the slag, V_s, indicated.

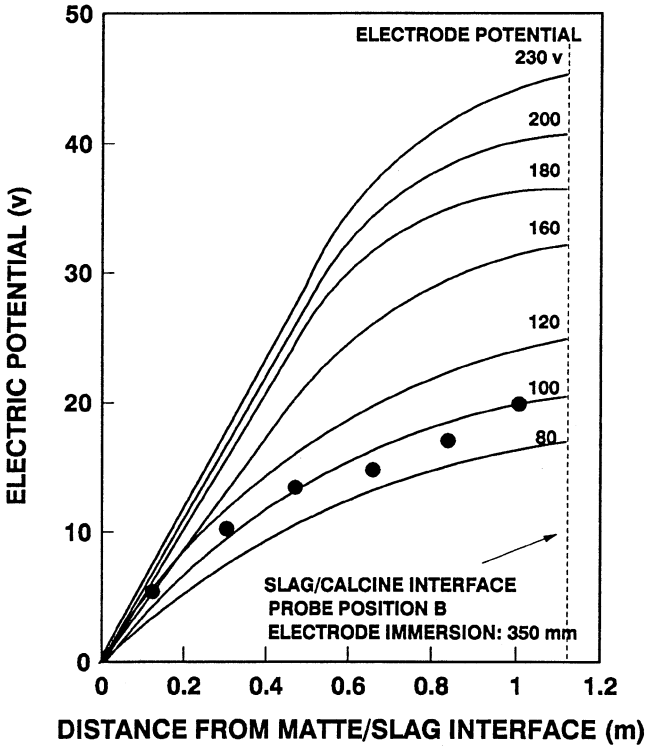

Fig. 10—Electric potential in the slag with respect to the matte as a function of distance from the matte at location B in furnace 2. The data correspond to 230 V applied to electrodes 2 and 3, 21 kA, and 12 MW between electrodes 2 and 3 with a slag depth of 300 mm. The lines were computed from the model for a slag depth of 350 mm, and the various potentials applied to the slag, V_s, indicated.

weak and the magnetic Reynolds number, Re_m, is small; hence, the fluid flow and current flux equations may be decoupled. The conservation of current may be written as

$$\nabla \cdot \mathbf{J} = \nabla \cdot (\sigma_s \nabla V) = 0 \qquad [2]$$

which is the familiar Laplace equation. As noted in Section IV, the temperature is uniform throughout most of the slag; thus, the conductivity will be uniform. If the conductivity is uniform, then it may be dropped from Eq. [2]. This equation was solved in three dimensions for various potentials in contact with the slag in Figures 8 through 10. The boundary conditions were the same as those described in Part II.

B. *Electric Potential Drop at Electrode Surface*

It is indeed striking that the measured electric potentials only agree with those calculated by Eq. [2] if the electric potential applied to the slag is 100 to 120 V less than that applied to the electrodes. The electric potential applied to the electrodes is measured above the furnace roof. Based on a conductivity of the Soderberg electrodes of 1.5×10^{-5} Ω m,[15] the resistance of an electrode is less than 0.1 mΩ, much lower than the resistance in the slag, which is of the order of 10 mΩ. Therefore, ohmic losses in the electrode are not responsible for the discrepancy.

The power associated with the difference in electric potential applied to the electrode and that experienced by the slag must be used in the furnace. If this were not the case, then the heat demands of the smelting processes could not be met. Therefore, one is left with the conclusion that the

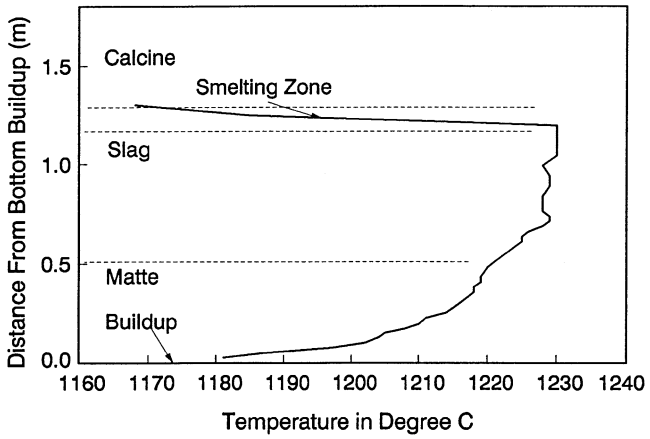

Fig. 11—Measured vertical temperature profile in the electric furnace at location A.

electric potential drop occurs in the melt, but is not associated with ohmic electric potential drop in the slag. The most plausible explanation for this finding is that the electric potential drop occurs at the surface of the electrode due to arcing. Each electrode is consumed at a rate of 5.8 kg/h at a smelting rate of 35 tonne/h by the reduction of oxides in the slag. The electrode carbon is most likely converted to carbon monoxide, yielding gas evolution rates of about 1.66×10^{-2} m^3/s at each electrode. The current must find its way through or around the gas. Given high temperatures, voltages, and current densities, the gas is likely ionized to create an arc or plasma. Figure 12 shows the equivalent

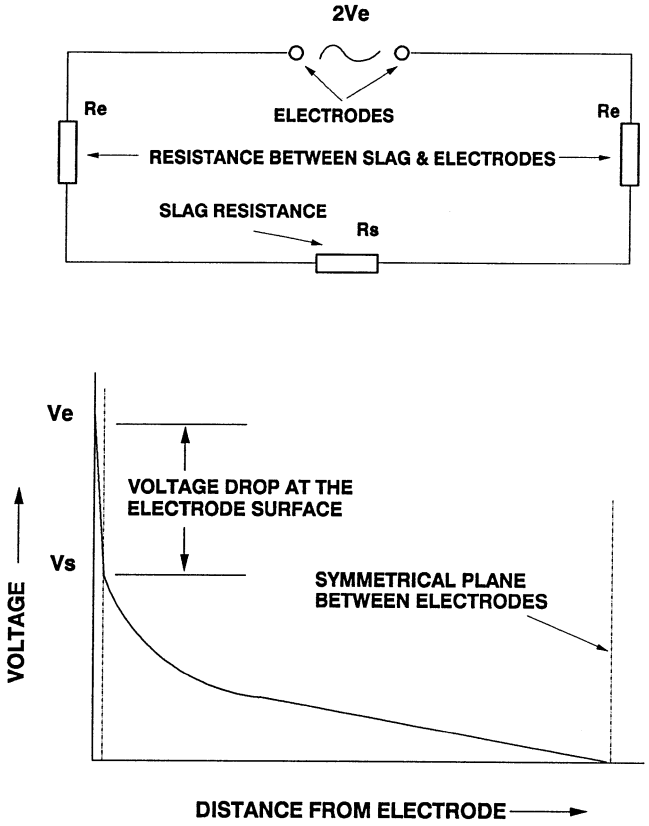

Fig. 12—Illustration of the equivalent circuit for the electric furnace showing that extra resistance at the electrode surface, R_e, results in a difference between the potential applied to the electrode, V_c, and the potential experienced by the slag, V_s.

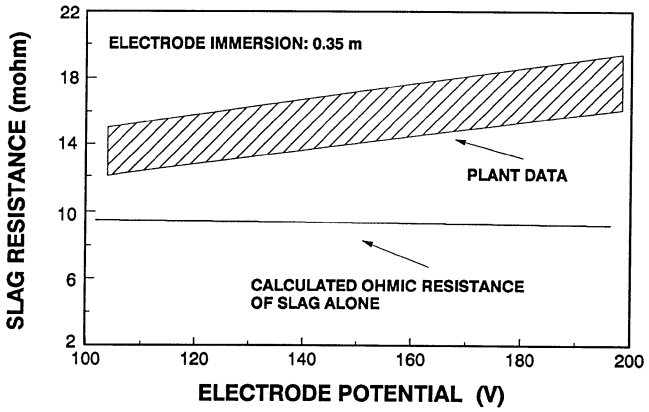

Fig. 13—Resistance as a function of the potential applied to the electrodes. The hatched region shows the range of resistance between electrodes measured in the plant. The line shows the ohmic resistance of the slag calculated with the model. The difference between the two is attributed to the arcing.

circuit for this phenomenon. There is a large electric potential drop at the electrode surface, $(V_c - V_s)$, due to the resistance between the slag and the electrodes. This electric potential drop will dissipate heat in the immediate vicinity of the electrodes. Figure 13 shows the resistance calculated for the slag alone with Eq. [2] compared with plant data. The calculated resistance of the slag alone is virtually constant, whereas the actual resistance increases with increasing electric potential applied to the electrodes. Apparently, the resistance of the arc increases with the applied potential. Figure 1 shows a comparison between the resistance of the slag alone and the measured resistance; the resistance due to arcing is not a strong function of immersion depth.

There is no published work on electric potential drops in carbon monoxide arcs; recent unpublished work at Mintek in South Africa[16] indicates that the potential drop over a 0.05-m gap of carbon monoxide in a smelting environment may be 70 to 190 V. While it is not possible to directly compare their work with the present, it demonstrates that arcing results in significant potential gradients.

As outlined in Section I, immersed-arc smelting is the only technique generally considered not to arc. The findings of the present investigation strongly suggest that there is an arc. However, it would be very difficult to make measurements near the electrode to obtain direct evidence of the arc and its shape. Furthermore, arcing may occur in other furnaces in which a graphite electrode is consumed because gas must be created, and under smelting conditions, it is likely ionized.

C. *Assessment of Analog Correlations*

Previous correlations[6,7,8] were developed by fitting regression equations to results obtained by the measurement of resistance in low-temperature, small-scale analog models of full-scale furnaces. In those models, there was no arcing at the electrodes, so these models cannot accurately portray the real electrodes in that respect.

In principle, there should be no difference between the data from the analog model and from the solution of the Laplace equation (Eq. [2]) for the determination of the ohmic portion of the resistance of the slag. Figure 1 shows a comparison between the analog correlations and the solution of Eq. [2] for the slag. The agreement is good for the deeper immersion depths, but is poor for shallow ones. This is probably a result of extrapolation of the correlations outside their range of validity. There are other potential problems with these correlations.

(1) In situations where the conductivity of the slag varies greatly, due to composition or temperature gradients, the constant conductivity of the analog correlations limits their applicability.
(2) Where the geometry is significantly different from the analog model, there may also be difficulties, such as the shallow immersion shown in Figure 1. The resistance is considerably larger in such cases, due to higher current density.

Therefore, it is preferable to solve the appropriate current equations rather than employ analog models, particularly when noting the ease with which this can be done with modern computers.

D. *The Measurement Technique*

This is the first time that the electric potential distribution in an electric smelting furnace has been reported. The probe designed for the electric potential measurement worked well. For the normal slag temperature of 1250 °C, the probe functioned in the slag for up to 1 hour. Its life was limited by erosion of the lowest electrode in the matte; erosion of the electrodes in the slag was negligible.

The accuracy of the electric potential measurement was affected by several factors such as the location of the electric potential probe and the choice of the ground point. The building ground was not suitable; much more stable readings were obtained when the electrode immersed in the matte was used as the reference. Some problems in reproducibility were encountered in exactly repositioning the probe at the same location due to the length of the probe. As will be shown in Part II, the electric potential is very sensitive to location.

VI. CONCLUSIONS

A novel multielectrode probe was developed to simultaneously measure the voltage at several locations in the slag of an electric furnace. Consequently, this is the first report of such measurements. By comparison with computed voltage distributions, it was deduced that there is a substantial voltage drop at the electrode interface, 100 to 120 V for applied potentials of 180 to 230 V for the Falconbridge furnace. This potential drop was attributed to the creation of an arc from the carbon monoxide evolved at the electrodes due to chemical erosion. Therefore, heat is evolved both at the electrode surface and in the bulk of the slag by ohmic heating. This improved understanding of the heat evolution was used in Part II.

ACKNOWLEDGMENTS

The authors are very grateful to Falconbridge, Limited, for funding this project and permitting publication of this article. The encouraging comments from Falconbridge personnel including Mr. Ian Cameron, Mr. Chai Tan, and Dr. Gary O'Connell are greatly appreciated. The assistance of Mr. Owen Kelly and Falconbridge's smelter technicians and furnace operators during the experiments is also gratefully acknowledged.

NOMENCLATURE

f_g	geometric factor of the electric furnace (l/m)
H_e	electrode immersion in slag (m)
H_s	slag thickness (m)
I	electrical current (A)
J	conduction current density (A/m^2)
L	length scale (m)
R_e	extra resistance between slag and electrode (ohm)
R_s	resistance of slag alone (ohm)
Re_m	magnetic Reynolds number, LU/α_m (—)
V_e	electric potential applied to electrode (V)
V_s	electric potential applied to slag (V)
U	velocity scale (m/s)
α_m	magnetic diffusivity $1/\sigma_s\mu_m$
σ_s	electrical conductivity of slag (mho/m)
μ_m	magnetic permeability (Henry/m)

REFERENCES

1. A.G. Matyas, R.C. Francki, K.M. Donaldson, and B. Wasmund: *CIM Bull.*, 1993, vol. 86 (972), pp. 92-99.
2. J.C. Taylor and H.R. Traulsen: *World Survey of Nonferrous Smelters*, Proc. Symp. on World Survey of Nonferrous Smelters at the TMS-AIME Annual Meeting, Jan. 25–29, 1988, Phoenix, AZ.
3. C. Diaz, B.R. Conard, C.E. O'Neill, and A.D. Dalvi: *CIM Bull.*, 1994, vol. 87 (98), pp. 62-68.
4. Y.Y. Sheng, G.A. Irons, and D.G. Tisdale: *Metall. Mater. Trans. B*, 1998, vol. 29B, pp. 85-94.
5. S.S. Attwood: *Electric and Magnetic Fields*, John Wiley & Sons, New York, NY, 1949, pp. 88 and 160.
6. J.A. Perssan and D.G. Treilhard: *J. Met.*, 1973, Jan., pp. 34-39.
7. R.C. Urquhart, M.S. Rennie, and C.C. Rabey: *Proc. Int. Symp. on Copper Extraction and Refining*, Feb. 22–26, 1976, Las Vegas, NV, A.K. Biswas and W.G. Davenport, eds., TMS-AIME, Warrendale, PA, 1976.
8. Q. Jiao and N.J. Themelis: *Metall. Trans. B*, 1988, vol. 19B, pp. 133-40.
9. G. O'Connell: ''Relationship between Slag Depth, Electrode Immersion, and Electrode Resistance in Falconbridge's Electric Furnaces,'' Inter-office Technical Report, Metallurgical Technology Centre. Falconbridge, Sudbury, ON, Canada, May 31, 1993.
10. Q. Jiao and N.J. Themelis: *Metall. Trans. B*, 1991, vol. 22B, pp. 183-92.
11. N.M. Stubina, G.H. Kaiura, H. Tseng, and J.M. Toguri: ''To Develop a Clean Smelting Process for Highly Roasted Copper-Nickel Calcines and to Improve Metal Recovery, Part D: Electrical Conductivity Measurements of Electric Furnace Smelting Slags,'' DSS File No. 15SQ.23440-3-9172, University of Toronto, Toronto, 1988.
12. N. Stubina, J. Chao, and C. Tan: *CIM Bull.*, 1994, June, pp. 57-61.
13. J.D. Kraus and K.R. Carver: *Electromagnetics*, 2nd ed. McGraw-Hill Book Company, New York, NY, 1973.
14. W.F. Hughes and F.J. Young: *The Electromagnetodynamics of Fluids*, Wiley, New York, NY, 1966.
15. J.R. Jones, M.A. Laughton, and M.G. Say: *Electrical Engineer's Reference Book*, 15th ed., Butterworth-Heinemann Ltd., Oxford, United Kingdom, 1993.
16. R. Jones: Mintek, Randburg, South Africa, private communication, 1996.